

DESY 96-201  
September 1996

## Color-Singlet and Color-Octet Contributions to $J/\psi$ Photoproduction\*

MICHAEL KRÄMER

*Deutsches Elektronen-Synchrotron DESY, D-22603 Hamburg, FRG*

I discuss the impact of color-octet contributions and higher-order QCD corrections on the cross section for inelastic  $J/\psi$  photoproduction. The theoretical predictions are compared with recent experimental data obtained at HERA.

### 1. Introduction

The production of heavy quarkonium states in high-energy collisions provides an important tool to study the interplay between perturbative and non-perturbative QCD dynamics. While the creation of heavy quarks in a hard scattering process can be calculated in perturbative QCD<sup>1</sup>, the subsequent transition to a physical bound state introduces non-perturbative aspects. A rigorous framework for treating quarkonium production and decays has recently been developed.<sup>2</sup> The factorization approach is based on the use of non-relativistic QCD<sup>3</sup> (NRQCD) to separate the short-distance parts from the long-distance matrix elements and explicitly takes into account the complete structure of the quarkonium Fock space. This formalism implies that so-called color-octet processes, in which the heavy-quark antiquark pair is produced at short distances in a color-octet state and subsequently evolves non-perturbatively into a physical quarkonium, should contribute to the cross section. It has recently been argued<sup>4,5</sup> that quarkonium production in hadronic collisions at the Tevatron can be accounted for by including color-octet processes and by adjusting the unknown long-distance color-octet matrix elements to fit the data.

In order to establish the phenomenological significance of the color-octet mechanism it is necessary to identify color-octet contributions in different production processes. Color-octet production of  $J/\psi$  particles has also been studied in the context of  $e^+e^-$  annihilation<sup>6</sup>,  $Z$  decays<sup>7</sup>, hadronic collisions at fixed-target experiments<sup>8,9</sup> and  $B$  decays<sup>10</sup>. Here, I review the impact of color-octet contributions and higher-order QCD corrections on the cross section for  $J/\psi$  photoproduction. The production of  $J/\psi$  particles in photon-proton collisions proceeds predominantly through photon-gluon fusion. Elastic/diffractive mechanisms<sup>11</sup> can be eliminated by measuring the  $J/\psi$  energy spectrum, described by the scaling variable  $z = p \cdot k_\psi / p \cdot k_\gamma$ ,

---

\*Talk presented at the Workshops 'QED and QCD in Higher Orders', Rheinsberg, Germany, April 21-26 and 'Quarkonium Physics', Chicago, USA, June 13-15, 1996; to appear in the proceedings.

with  $p, k_{\psi, \gamma}$  being the momenta of the proton and  $J/\psi, \gamma$  particles, respectively. In the proton rest frame,  $z$  is the ratio of the  $J/\psi$  to  $\gamma$  energy,  $z = E_{\psi}/E_{\gamma}$ . For elastic/diffractive events  $z$  is close to one; a clean sample of inelastic events can be obtained in the range  $z \lesssim 0.9$ .

According to the NRQCD factorization formalism, the inclusive cross section for  $J/\psi$  photoproduction can be expressed as a sum of terms, each of which factors into a short-distance coefficient and a long-distance matrix element:

$$d\sigma(\gamma + g \rightarrow J/\psi + X) = \sum_n d\hat{\sigma}(\gamma + g \rightarrow c\bar{c}[n] + X) \langle \mathcal{O}^{J/\psi}[n] \rangle \quad (1)$$

Here,  $d\hat{\sigma}$  denotes the short-distance cross section for producing an on-shell  $c\bar{c}$ -pair in a color, spin and angular-momentum state labelled by  $n$ . The NRQCD matrix elements  $\langle \mathcal{O}^{J/\psi}[n] \rangle \equiv \langle 0 | \mathcal{O}^{J/\psi}[n] | 0 \rangle$  give the probability for a  $c\bar{c}$ -pair in the state  $n$  to form the  $J/\psi$  particle. The relative importance of the various terms in (1) can be estimated by using NRQCD velocity scaling rules.<sup>12</sup> For  $v \rightarrow 0$  ( $v$  being the average velocity of the charm quark in the  $J/\psi$  rest frame) each of the NRQCD matrix elements scales with a definite power of  $v$  and the general expression (1) can be organized into an expansion in powers of  $v^2$ .

## 2. Color-singlet contribution

At leading order in  $v^2$ , eq.(1) reduces to the standard factorization formula of the color-singlet model<sup>13</sup>. The short-distance cross section is given by the subprocess

$$\gamma + g \rightarrow c\bar{c}[\underline{\mathbf{1}}, {}^3S_1] + g \quad (2)$$

shown in Fig.1a, with  $c\bar{c}$  in a color-singlet state (denoted by  $\underline{\mathbf{1}}$ ), zero relative velocity, and spin/angular-momentum quantum numbers  ${}^{2S+1}L_J = {}^3S_1$ . Up to corrections of  $\mathcal{O}(v^4)$ , the color-singlet NRQCD matrix element is related to the  $J/\psi$  wave function at the origin through  $\langle \mathcal{O}^{J/\psi}[\underline{\mathbf{1}}, {}^3S_1] \rangle \approx (9/2\pi)|\varphi(0)|^2$  and can be extracted from the measurement of the  $J/\psi$  leptonic decay width or calculated within potential models. Relativistic corrections due to the motion of the charm quarks in the  $J/\psi$  bound state enhance the large- $z$  region, but can be neglected in the inelastic domain.<sup>14</sup> The calculation of the higher-order perturbative QCD corrections to the short-distance cross section (2) has been performed recently.<sup>15,16</sup> Generic diagrams which build up the cross section in next-to-leading order (NLO) are depicted in Fig.1. Besides the usual self-energy diagrams and vertex corrections for photons and gluons (b), one encounters box diagrams (c), the splitting of the final-state gluon into gluon and light quark-antiquark pairs, as well as diagrams renormalizing the initial state parton densities (e). Inclusion of the NLO corrections reduces the scale dependence of the theoretical prediction and increases the cross section significantly, depending in detail on the  $\gamma p$  energy and the choice of parameters.<sup>16</sup> Details of the calculation and a comprehensive analysis of total cross sections and differential distributions for the energy range of the fixed-target experiments and for  $J/\psi$  photoproduction at HERA can be found elsewhere.<sup>16</sup>

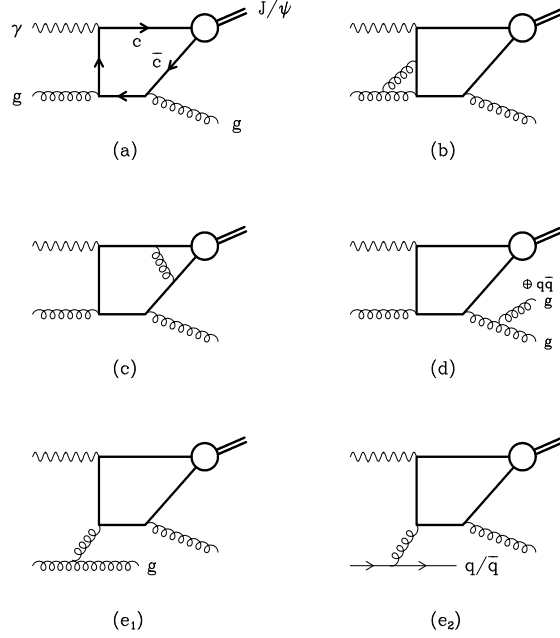


Fig. 1. Generic diagrams for  $J/\psi$  photoproduction via the color-singlet channel: (a) leading order contribution; (b) vertex corrections; (c) box diagrams; (d) splitting of the final state gluon into gluon or light quark-antiquark pairs; (e) diagrams renormalizing the initial-state parton densities.

### 3. Color-octet contributions

Color-octet configurations are produced at leading order in  $\alpha_s$  through the  $2 \rightarrow 1$  parton processes<sup>17,18,19</sup>

$$\begin{aligned} \gamma + g &\rightarrow c\bar{c}[\underline{8}, {}^1S_0] \\ \gamma + g &\rightarrow c\bar{c}[\underline{8}, {}^3P_{0,2}] \end{aligned} \quad (3)$$

shown in Fig.2a. Due to kinematical constraints, the leading color-octet terms will only contribute to the upper endpoint of the  $J/\psi$  energy spectrum,  $z \approx 1$  and  $p_\perp \approx 0$ ,  $p_\perp$  being the  $J/\psi$  transverse momentum. Color-octet configurations which contribute to inelastic  $J/\psi$  photoproduction  $z \leq 0.9$  and  $p_\perp \geq 1$  GeV are produced through the subprocesses<sup>17,19</sup>

$$\begin{aligned} \gamma + g &\rightarrow c\bar{c}[\underline{8}, {}^1S_0] + g \\ \gamma + g &\rightarrow c\bar{c}[\underline{8}, {}^3S_1] + g \\ \gamma + g &\rightarrow c\bar{c}[\underline{8}, {}^3P_{0,1,2}] + g \end{aligned} \quad (4)$$

as shown in Fig.2b. Light-quark initiated contributions are strongly suppressed at HERA energies and can safely be neglected.

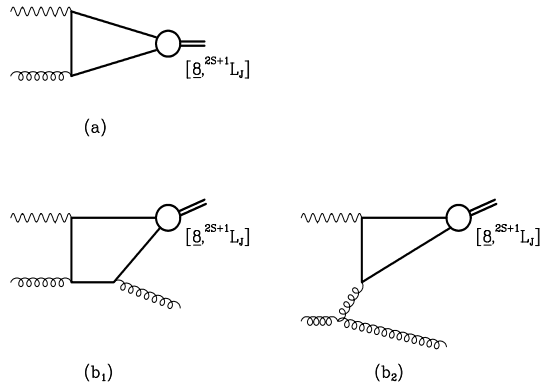


Fig. 2. Generic diagrams for  $J/\psi$  photoproduction via color-octet channels: (a) leading color-octet contributions; (b) color-octet contributions to inelastic  $J/\psi$  production.

The transition of the color-octet  $c\bar{c} [\underline{8}, {}^{2S+1}L_J]$  pair into a physical  $J/\psi$  state through the emission of non-perturbative gluons is described by the long-distance matrix elements  $\langle \mathcal{O}^{J/\psi} [\underline{8}, {}^{2S+1}L_J] \rangle$ . They have to be obtained from lattice simulations<sup>20</sup> or measured directly in some production process. According to the velocity scaling rules of NRQCD, the color-octet matrix elements associated with  $S$ -wave quarkonia should be suppressed by a factor of  $v^4$  compared to the leading color-singlet matrix element.<sup>†</sup> Color-octet contributions to  $J/\psi$  photoproduction can thus become important only if the corresponding short-distance cross sections are enhanced as compared to the color-singlet process. Color-octet matrix elements have been fitted to prompt  $J/\psi$  data from CDF<sup>24</sup> and found to be  $\mathcal{O}(10^{-2} \text{ GeV}^3)$ , consistent with the NRQCD velocity scaling rules.<sup>4,5</sup> Meanwhile, fit values for color-octet matrix elements have also been obtained from analyses of quarkonium production in hadronic collisions at fixed-target experiments<sup>9</sup>,  $J/\psi$  photoproduction at the elastic peak<sup>18</sup> and  $J/\psi$  production in  $B$  decays<sup>10</sup>. The results seem to indicate that the values for the color-octet matrix elements extracted from the Tevatron data at moderate  $p_\perp$  are too large; they should however be considered with some caution since significant higher-twist corrections are expected to contribute in the small- $p_\perp$  region probed at fixed target experiments and in elastic  $J/\psi$  photoproduction. Moreover, the comparison between the different analyses is rendered difficult by the fact that the color-octet matrix elements can in general only be extracted in certain linear combinations which depend on the reaction under consideration, see Sec.4.

#### 4. $J/\psi$ photoproduction at HERA

The production of  $J/\psi$  particles in high energy  $ep$  collisions at HERA is domi-

<sup>†</sup>In the case of  $P$ -wave quarkonia, color-singlet and color-octet matrix elements contribute at the same order in  $v$ .<sup>21</sup> Photoproduction of  $P$ -wave states is, however, suppressed compared with  $J/\psi$  states, by two orders of magnitude at HERA.<sup>22,23</sup>

nated by photoproduction events where the electron is scattered by a small angle producing photons of almost zero virtuality. The measurements at HERA provide information on the dynamics of  $J/\psi$  photoproduction in a wide kinematical region,  $30 \text{ GeV} \lesssim \sqrt{s_{\gamma p}} \lesssim 200 \text{ GeV}$ , corresponding to initial photon energies in a fixed-target experiment of  $450 \text{ GeV} \lesssim E_\gamma \lesssim 20,000 \text{ GeV}$ . Due to kinematical constraints, the leading color-octet processes (3) contribute only to the upper endpoint of the  $J/\psi$  energy spectrum,  $z \approx 1$  and  $p_\perp \approx 0$ . The color-singlet and color-octet predictions (3) have been compared to experimental data<sup>25</sup> obtained in the region  $z \geq 0.95$  and  $p_\perp \leq 1 \text{ GeV}$ .<sup>17</sup> Since the factorization approach cannot be used to describe the exclusive elastic channel  $\gamma + p \rightarrow J/\psi + p$ , elastic contributions had been subtracted from the data sample. It was shown that the large cross section predicted by using color-octet matrix elements as extracted from the Tevatron fits appears to be in conflict with the experimental data. It is, however, difficult to put strong upper limits for the octet terms from a measurement of the total cross section in the region  $z \approx 1$  and  $p_\perp \approx 0$  since the overall normalization of the theoretical prediction depends strongly on the choice for the charm quark mass and the QCD coupling. Moreover, diffractive production mechanisms which cannot be calculated within perturbative QCD might contaminate the region  $z \approx 1$  and make it difficult to extract precise information on the color-octet contributions. Finally, it has been argued that sizable higher-twist effects are expected to contribute in the region  $p_\perp \lesssim 1 \text{ GeV}$ , which cause the breakdown of the factorization formula (1).<sup>26</sup>

It is therefore more appropriate to study  $J/\psi$  photoproduction in the inelastic region  $z \leq 0.9$  and  $p_\perp \geq 1 \text{ GeV}$  where no diffractive channels contribute and where the general factorization formula (1) and perturbative QCD calculations should be applicable. Adopting the NRQCD matrix elements as extracted from the fits to prompt  $J/\psi$  data at the Tevatron one finds that color-octet and color-singlet contributions to the inelastic cross section are predicted to be of comparable size.<sup>17,19</sup> The short-distance factors of the  $[\underline{8}, ^1S_0]$  and  $[\underline{8}, ^3P_{0,2}]$  channels are strongly enhanced as compared to the color-singlet term and partly compensate the  $\mathcal{O}(10^{-2})$  suppression of the corresponding non-perturbative matrix elements. In contrast, the contributions from the  $[\underline{8}, ^3S_1]$  and  $[\underline{8}, ^3P_1]$  states are suppressed by more than one order of magnitude. Since color-octet and color-singlet processes contribute at the same order in  $\alpha_s$ , the large size of the  $[\underline{8}, ^1S_0]$  and  $[\underline{8}, ^3P_{0,2}]$  cross sections could not have been anticipated from naive power counting and demonstrates the crucial dynamical role played by the bound state quantum numbers.<sup>27</sup> As for the total inelastic cross section, the linear combination of the color-octet matrix elements  $\langle \mathcal{O}^{J/\psi} [\underline{8}, ^1S_0] \rangle$  and  $\langle \mathcal{O}^{J/\psi} [\underline{8}, ^3P_0] \rangle$  that is probed at HERA is almost identical to that extracted from the Tevatron fits at moderate  $p_\perp$ , independent of  $\sqrt{s_{\gamma p}}$ .<sup>‡</sup> The Tevatron results can thus be used to make predictions for color-octet contributions to the total inelastic  $J/\psi$  photoproduction cross section without further ambiguities. However, taking into account the uncertainty due to the value of the charm

<sup>‡</sup>At leading order in  $v^2$ , the  $P$ -wave matrix elements are related by heavy-quark spin symmetry,  $\langle \mathcal{O}^{J/\psi} [\underline{8}, ^3P_J] \rangle \approx (2J+1) \langle \mathcal{O}^{J/\psi} [\underline{8}, ^3P_0] \rangle$ .

quark mass and the strong coupling, the significance of color-octet contributions cannot be deduced from the analysis of the absolute  $J/\psi$  production rates. In fact, the experimental data can be accounted for by the color-singlet channel alone, once higher-order QCD corrections are included and the theoretical uncertainties due to variation of the charm quark mass and the strong coupling are taken into account, as demonstrated at the end of this section. The same statement holds true for the transverse momentum spectrum, since, at small and moderate  $p_\perp$ , both color-singlet and color-octet contributions are almost identical in shape. At large transverse momenta,  $p_\perp \gtrsim 10$  GeV, charm quark fragmentation dominates over the photon-gluon fusion process.<sup>28,29</sup> In contrast to what was found at the Tevatron<sup>30</sup>, gluon fragmentation into color-octet states is suppressed over the whole range of  $p_\perp$  in the inelastic region  $z \lesssim 0.9$ .<sup>29</sup>

A distinctive signal for color-octet processes should, however, be visible in the  $J/\psi$  energy distribution  $d\sigma/dz$ .<sup>17</sup> The linear combination of color-octet matrix elements that is probed by the  $J/\psi$  energy distribution does, however, depend on the value of  $z$ . Therefore, one cannot directly use the Tevatron fits but has to allow the individual color-octet matrix elements to vary in certain ranges, constrained by the value extracted for the linear combination. It has in fact been argued that the color-octet matrix element  $\langle \mathcal{O}^{J/\psi} [\underline{8}, {}^3P_0] \rangle$  could be negative due to the subtraction of power ultraviolet divergences.<sup>31</sup> In contrast, the matrix element  $\langle \mathcal{O}^{J/\psi} [\underline{8}, {}^1S_0] \rangle$  is free of power divergences and its value is thus always positive. Accordingly, I have allowed  $\langle \mathcal{O}^{J/\psi} [\underline{8}, {}^3P_0] \rangle/m_c^2$  to vary in the range  $[-0.01, 0.01]$  GeV<sup>3</sup> and determined the value of the matrix element  $\langle \mathcal{O}^{J/\psi} [\underline{8}, {}^1S_0] \rangle$  from the linear combination extracted at the Tevatron.<sup>§</sup> The result is shown in Fig.3(a) where I have plotted (leading-order) color-singlet and color-octet contributions at a typical HERA energy of  $\sqrt{s_{\gamma p}} = 100$  GeV in the restricted range  $p_\perp \geq 1$  GeV, compared to recent experimental data from H1<sup>25</sup> and preliminary data from ZEUS<sup>32</sup>. The hatched error band indicates how much the color-octet cross section is altered if  $\langle \mathcal{O}^{J/\psi} [\underline{8}, {}^3P_0] \rangle/m_c^2$  varies in the range  $[-0.01, 0.01]$  GeV<sup>3</sup>, where the lower bound corresponds to  $\langle \mathcal{O}^{J/\psi} [\underline{8}, {}^3P_0] \rangle/m_c^2 = -0.01$  GeV<sup>3</sup>. Since the shape of the distribution is almost insensitive to higher-order QCD corrections or to the uncertainty induced by the choice for  $m_c$  and  $\alpha_s$ , the analysis of the  $J/\psi$  energy spectrum  $d\sigma/dz$  should provide a clean test for the underlying production mechanism. From Fig.3 one can conclude that the shape predicted by the color-octet contributions is not supported by the experimental data. The discrepancy with the data can only be removed when reducing the relative weight of the color-octet contributions by at least a factor of five.<sup>17</sup> Let me emphasize that the rise of the cross section towards large  $z$  predicted by the color-octet mechanism is not sensitive to the small- $p_\perp$  region and thus not affected by the collinear divergences which show up at the endpoint  $z = 1$  and  $p_\perp = 0$ . This is demonstrated in Fig.3(b) where I show color-singlet and color-octet contributions to the  $J/\psi$  energy distribution for  $p_\perp > 5$  GeV. It will be

<sup>§</sup>Note that, given  $\langle \mathcal{O}^{J/\psi} [\underline{8}, {}^1S_0] \rangle \lesssim 0.1$  GeV<sup>3</sup> as required by the velocity scaling rules, a value  $\langle \mathcal{O}^{J/\psi} [\underline{8}, {}^3P_0] \rangle/m_c^2 \lesssim -0.01$  GeV<sup>3</sup> would be in contradiction with the Tevatron fits.

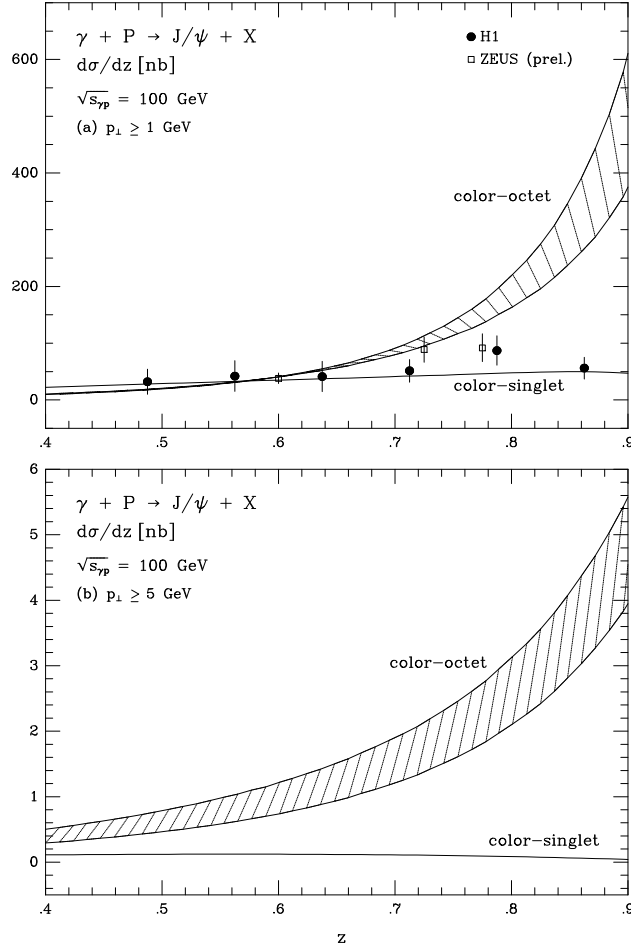


Fig. 3. Color-singlet and color-octet contributions to the  $J/\psi$  energy distribution  $d\sigma/dz$  at the photon-proton centre of mass energy  $\sqrt{s_{\gamma p}} = 100$  GeV integrated in the range (a)  $p_{\perp} \geq 1$  GeV and (b)  $p_{\perp} \geq 5$  GeV compared to experimental data<sup>25,32</sup>.

very interesting to compare these predictions with data to be expected in the future at HERA. Let me finally mention that the shape of the  $J/\psi$  energy distribution could be influenced by the emission of soft gluons from the intermediate color-octet state.<sup>9</sup> While this effect, which cannot be predicted within the NRQCD factorization approach, might be significant at the elastic peak, it is by no means clear if and in which way it could affect the inelastic region  $z \lesssim 0.9$  and  $p_{\perp} \gtrsim 1$  GeV. In fact, if soft gluon emission were important, it should also result in a feed-down of the leading color-octet contributions (3) into the inelastic domain, thereby increasing the discrepancy between the color-octet cross section and the data in the large- $z$  region.

For the remainder of this section, I will demonstrate that the experimental results on differential distributions and total cross sections are well accounted for

by the color-singlet channel alone including higher-order QCD corrections. This can e.g. be inferred from Fig.4 where I compare the NLO color-singlet prediction for the  $J/\psi$  transverse momentum distribution<sup>16</sup> with recent results from H1<sup>25</sup>. Note

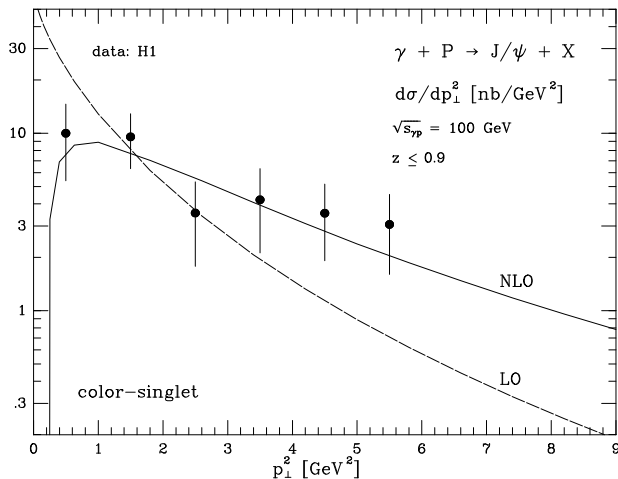


Fig. 4. LO and NLO color-singlet prediction for the  $J/\psi$  transverse momentum spectrum  $d\sigma/dp_{\perp}^2$  at the photon-proton centre of mass energy  $\sqrt{s_{\gamma p}} = 100$  GeV integrated in the range  $z \leq 0.9$  compared to experimental data<sup>25</sup>.

that the inclusion of higher-order QCD corrections is crucial to describe the shape of the  $p_{\perp}$  distribution. However, a detailed analysis of the transverse momentum spectrum reveals that the fixed-order perturbative QCD calculation is not under proper control in the limit  $p_{\perp} \rightarrow 0$ , Fig.4. No reliable prediction can be made in the small- $p_{\perp}$  domain without resummation of large logarithmic corrections caused by multiple gluon emission. If the region  $p_{\perp} \leq 1$  GeV is excluded from the analysis, the next-to-leading order color-singlet prediction accounts for the energy dependence of the cross section and for the overall normalization, Fig. 5. The sensitivity of the prediction to the small- $x$  behaviour of the gluon distribution is however not very distinctive, since the average momentum fraction of the partons  $\langle x \rangle$  is shifted to larger values when excluding the small- $p_{\perp}$  region.

## 5. Conclusion

I have discussed color-singlet and color-octet contributions to the production of  $J/\psi$  particles in photon-proton collisions, including higher-order QCD corrections to the color-singlet channel. A comparison with photoproduction data obtained at fixed-target experiments<sup>16</sup> and the  $ep$  collider HERA reveals that the  $J/\psi$  energy spectrum and the slope of the transverse momentum distribution are adequately accounted for by the next-to-leading order color-singlet prediction in the inelastic region  $p_{\perp} \gtrsim 1$  GeV and  $z \lesssim 0.9$ . Taking into account the uncertainty due to variation of the charm quark mass and the strong coupling, one can conclude that

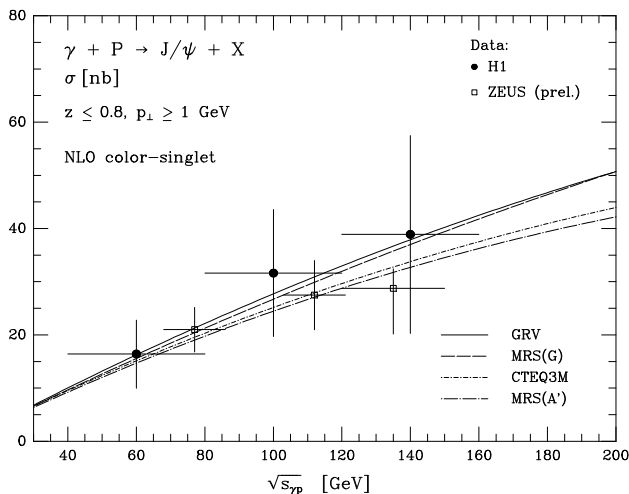


Fig. 5. NLO color-singlet prediction for the total inelastic  $J/\psi$  photoproduction cross section as a function of the photon-proton energy for different parametrizations<sup>33</sup> of the parton distribution in the proton compared to experimental data<sup>25,32</sup>.

the normalization too appears to be under semi-quantitative control. Higher-twist effects<sup>34</sup> must be included to improve the quality of the theoretical analysis further. Distinctive signatures for color-octet processes should be visible in the shape of the  $J/\psi$  energy distribution. However, these predictions appear at variance with recent experimental data obtained at HERA indicating that the values of the color-octet matrix elements  $\langle \mathcal{O}^{J/\psi} [\underline{8}, ^1S_0] \rangle$  and  $\langle \mathcal{O}^{J/\psi} [\underline{8}, ^3P_0] \rangle$  are considerably smaller than suggested by the fits to Tevatron data at moderate  $p_{\perp}$ . Support is added to this result by recent analyses on  $J/\psi$  production in hadronic collisions at fixed-target energies<sup>9</sup> and  $B$  decays<sup>10</sup>. Clearly, much more effort, both theoretical and experimental, is needed to establish the phenomenological significance of color-octet contributions to  $J/\psi$  production and to proof the applicability of the NRQCD factorization approach to charmonium production in hadronic collisions at moderate transverse momentum.

### Acknowledgements

I wish to thank Martin Beneke, Eric Braaten, Matteo Cacciari, Sean Fleming and Arthur Hebecker for useful discussions.

### References

1. J.C. Collins, D.E. Soper, and G. Sterman, Nucl. Phys. **B263** (1986) 37.
2. G.T. Bodwin, E. Braaten, and G.P. Lepage, Phys. Rev. **D51** (1995) 1125.
3. W.E. Caswell and G.P. Lepage, Phys. Lett. **B167** (1986) 437.
4. E. Braaten and S. Fleming, Phys. Rev. Lett. **74** (1995) 3327; M. Cacciari, M. Greco, M.L. Mangano, and A. Petrelli, Phys. Lett. **B356** (1995) 560.

5. P. Cho and A.K. Leibovich, Phys. Rev. **D53** (1996) 150 and *ibid.* **53** (1996) 6203.
6. E. Braaten and Y.-Q. Chen, Phys. Rev. Lett. **76** (1996) 730.
7. K. Cheung, W.-Y. Keung, and T.C. Yuan, Phys. Rev. Lett. **76** (1996) 877; P. Cho, Phys. Lett. **B368** (1996) 171.
8. W.-K. Tang and M. Vanttinen, Phys. Rev. **D53** (1996) 4851 and *ibid.* **54** (1996) 4349. S. Fleming and I. Maksymyk, Phys. Rev. **D54** (1996) 3608; S. Gupta and K. Sridhar, TIFR-TH-96-04 (hep-ph/9601349);
9. M. Beneke and I.Z. Rothstein, Phys. Rev. **D54** (1996) 2005.
10. P. Ko, J. Lee, and H.S. Song, Phys. Rev. **D53** (1996) 1409; S. Fleming, O.F. Hernández, I. Maksymyk, and H. Nadeau, MADPH-96-953 (hep-ph/9608413).
11. A. Donnachie and P.V. Landshoff, Phys. Lett. **B348** (1995) 213; M.G. Ryskin, R.G. Roberts, A.D. Martin, and E.M. Levin, DTP-95-96 (hep-ph/9511228); T. Ahmed et al. [H1 Collab.], Phys. Lett. **B338** (1994) 507; M. Derrick et al. [ZEUS Collab.], Phys. Lett. **B350** (1995) 120.
12. G.P. Lepage, L. Magnea, C. Nakhleh, U. Magnea, and K. Hornbostel, Phys. Rev. **D46** (1992) 4052.
13. E.L. Berger and D. Jones, Phys. Rev. **D23** (1981) 1521; R. Baier and R. Rückl, Phys. Lett. **102B** (1981) 364; for a recent review see also G.A. Schuler, CERN-TH.7170/94 (hep-ph/9403387).
14. W.Y. Keung and I.J. Muzinich, Phys. Rev. **D27** (1983) 1518; H. Jung, D. Krücker, C. Greub, and D. Wyler, Z. Phys. **C60** (1993) 721; H. Khan and P. Hoodbhoy, Phys. Lett. **B382** (1996) 189.
15. M. Krämer, J. Zunft, J. Steegborn, and P.M. Zerwas, Phys. Lett. **B348** (1995) 657.
16. M. Krämer, Nucl. Phys. **B459** (1996) 3.
17. M. Cacciari and M. Krämer, Phys. Rev. Lett. **76** (1996) 4128.
18. J. Amundson, S. Fleming, and I. Maksymyk, UTTG-10-95 (hep-ph/9601298).
19. P. Ko, J. Lee, and H.S. Song, Phys. Rev. **D54** (1996) 4312.
20. G.T. Bodwin, D.K. Sinclair, and S. Kim, ANL-HEP-PR-96-28 (hep-lat/9605023).
21. G.T. Bodwin, E. Braaten, and G.P. Lepage, Phys. Rev. **D46** (1992) R1914.
22. J.P. Ma, Nucl. Phys. **B460** (1996) 109.
23. M. Cacciari and M. Krämer, to appear in the proceedings of the workshop ‘Future physics at HERA’, eds. G. Ingelman, A. De Roeck and R. Klanner.
24. F. Abe et al. [CDF Collab.], Phys. Rev. Lett. **69** (1992) 3704; A. Sansoni, [CDF Collab.], FERMILAB-CONF-95/263-E.
25. S. Aid et al. [H1 Collab.], Nucl. Phys. **B472** (1996) 3.
26. E. Braaten, S. Fleming, and T.C. Yuan, OHSTPY-HEP-T-96-001 (hep-ph/9602374); E. Braaten and Y.-Q. Chen, Phys. Rev. **D54** (1996) 3216.
27. R. Baier and R. Rückl, Z. Phys. **C19** (1983) 251.
28. V.A. Saleev, Mod. Phys. Lett. **A9** (1994) 1083.
29. R. Godbole, D.P. Roy, and K. Sridhar, Phys. Lett. **B373** (1996) 328.
30. M. Cacciari and M. Greco, Phys. Rev. Lett. **73** (1994) 1586; E. Braaten, M.A. Doncheski, S. Fleming, and M.L. Mangano, Phys. Lett. **B333** (1994) 548; D.P. Roy and K. Sridhar, Phys. Lett. **B339** (1994) 141.
31. E. Braaten, private communication.
32. M. Derrick et al. [ZEUS Collab.], presented by L. Stanco at the International Workshop on Deep Inelastic Scattering, Rome, April 1996.
33. M. Glück, E. Reya, and A. Vogt, Z. Phys. **C67** (1995) 433; A.D. Martin, G. Roberts, and W.J. Stirling, Phys. Lett. **B354** (1995) 155; H.L. Lai, J. Botts, J. Huston, J.G. Morfin, J.F. Owens, J.W. Qiu, W.K. Tung, and H. Weerts, Phys. Rev. **D51** (1995) 4763.
34. S.J. Brodsky, W.-K. Tang, and P.Hoyer, Phys. Rev. **D52** (1995) 6285.